STUDY ON ARCTIC MELT POND FRACTION RETRIEVAL ALGORITHM USING MODIS DATA

J. Su[1,2*], P. Yu[1,3], Y. Qin[1,2], G. Zhang[1], M. Wang[1,4]

[1] Physical Oceanography Laboratory, Ocean University of China, Qingdao 266100, China
[2] Qingdao National Laboratory for Marine Science and Technology, Qingdao, 266100, China
[3] Institute for Atmospheric and Earth System Research/Physics, Faculty of Science, University of Helsinki, Helsinki, Finland
[4] Earth Observation and Modelling, Department of Geography, Kiel University, Kiel, Germany

Commission III

KEY WORDS: Arctic, melt pond fraction, retrieval algorithm, MODIS

ABSTRACT:

During spring and summer, melt ponds appear on the sea ice surface in the Arctic and play an important role in sea ice-albedo feedback effect. The melt pond fraction (MPF) can be retrieved using multi-band linear equations, but the calculation is complicated by the ill-conditioned reflectance matrix. In this paper, we calculated the condition numbers which represent the degree of the ill-conditioned reflectance matrix in the results of the MPF from a MODIS-based unmixing algorithm. The condition number is introduced here as a criterion for the sensitivity of the solution in the system to the error in the input value. By combining 3 bands among 5 visible and near-infrared bands of MODIS data, the results show that the three-band combination with the lowest sensitivity to the error of input is B245. To improve the algorithm, we introduce pre-processing to remove open water from the four surface types and then remove one reflectance equation from the original set. The best two-band combination algorithm is B15. Compared with the discrimination results from Landsat5-TM, the RMS is 0.14. This algorithm is applied in pan-Arctic scale, the MPF results are larger than that from University of Hamburg, especially in the Pacific sector.

1. INTRODUCTION

The albedo of melt ponds is between open water and sea ice. Melt ponds occupy a large fraction of the Arctic sea ice surface during spring and summer. The fraction and distribution of melt ponds play an important role in the sea ice-albedo feedback. Accurate melt pond fraction (MPF) data is critical for calculating solar radiation absorption in sea ice and ocean underneath.

Optical imagery is one of the primary sources to acquire MPF information. Observations have shown that the melt pond fraction can vary by more than 60% throughout the melt season and by up to 40% depending on years and locations (Polashenski et al., 2012; Landy et al., 2014; 2015). The Arctic melt ponds are dominated by small-sized ones (normally <200m^2) (Perovich et al., 2002; Tschudi et al., 2001; Lu et al., 2010). If the sizes of several melt ponds are larger than the pixel area of high-resolution optical imagery, a basic principle of retrieving MPF is used to discriminate pixels of snow/bare ice from open water and melt ponds, based on their different reflective properties (Markus et al., 2002; Rösel et al., 2011). For the medium-resolution sensors with 500m or 1km resolution, such as MODerate-resolution Imaging Spectroradiometer (MODIS), unmixing is certainly required. Although the calculation of the unmixing formula has problems (for example, when the equations are approximately linearly correlated to each other, ill-conditioned reflectance matrix will occur and the solutions are sensitive to errors in the input data), its advantage of broad coverage and daily repeat-frequency gives people the reason to use it for the research of Arctic variability and to improve the algorithm constantly.

The wildly used MODIS MPF product (Rösel et al., 2012, hereafter called R12) is based on a spectral unmixing procedure which first proposed by Tschudi et al. (2008), hereafter called T08. In the R12 algorithm, they applied a neural network to determine the coefficients of algorithm. Zege et al. (2015) developed a MPF algorithm using the analytical solution of optical thickness layer to describe the albedo of white ice to calculate the BRDF of white ice and melt ponds based on MEdium-Resolution Imaging Spectrometer (MERIS) data. This algorithm is more physically grounded than that of R12. However, their MPF results only cover part of the Arctic (Istomina et al., 2015).

In this paper we calculated the condition numbers which represent the degree of the ill-conditioned reflectance matrix happened in the results of the MPF based on T08 using MODIS data. Some improvements were made to reduce the sensitivity of the linear functions. And the results were compared with Landsat data as well as the MPF product from Hamburg University (Rösel et al., 2012).

2. DATA

MODIS surface reflectance data (MOD09 and MOD09A1) is used as basic dataset. MOD09 is L2 data and stored by strips. MOD09 provides MODIS surface reflectance for bands 1 and 2 (at 250m), bands 1-7 (at 500 m), bands 1-16 (at 1 km resolution) and geographic information. MOD09 TrueColor image (Figure 1) which covered Beaufort Sea on June 13, 2004 was used following the original case of T08. MOD09A1 is L3 grid data. Each MOD09A1 pixel includes the best possible L2G observation during an 8-day period as selected on the basis of

high observation coverage, low view angle. MOD09A1 contains bands 1-7 at 500-meter resolution with quality control. It provides the broad coverage of the whole Arctic data and has removed the strong effects of cloud, shadow, and aerosol compared with MOD09GA data, which is a grid track data.

The MPF product from University Hamburg (R12) is used to compare with these results in the year of 2007. Landsat5-TM data archived by the United States Geological Survey (USGS) serves as the high-resolution data for validating MODIS products.

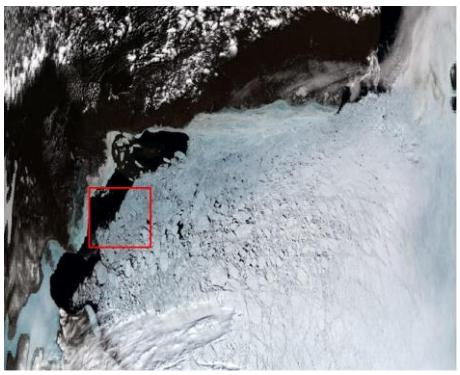

Fig. 1 TureColor image of MODIS band 2 at Beaufort Sea (June 13, 2004)

3. METHOD

Th spatial resolution of MODIS data is 500m, much greater than the common melt pond size. Therefore, it is impossible to resolve individual pond directly in almost all cases. T08 algorithm assumes every surface type in a given pixel reflects independently, and the total energy they reflect at a given wavelength determines the pixel's corresponding reflectance. For each pixel,

$$[\sum a_i r_i = R]_k \quad (1)$$

where a_i = the coverage of each surface type
r_i = each surface type's reflectance
R = the "in-situ" reflectance from MOD09 data
i = indicates surface types
k = MODIS bands

In the original algorithm design, there are 4 types: snow, ice, melt pond, and water. This means 4 independent linear equations are needed to solve for coverage. The sum of all the types' coverage should be 1,

$$\sum a_i = 1 \quad (a_i \geq 0) \quad (2)$$

The other 3 equations are acquired from bands 1, 2, 3 and the reflectance coefficients r_i are from in-situ observations. According to T08, the reflectance coefficient matrix is as following:

$$\begin{bmatrix} 0.16 & 0.75 & 0.95 & 0.08 \\ 0.07 & 0.56 & 0.87 & 0.08 \\ 0.22 & 0.76 & 0.95 & 0.08 \\ 1.00 & 1.00 & 1.00 & 1.00 \end{bmatrix}$$

Where columns represent melt pond, ice, snow and water (from left to right), and rows denote reflectance coefficients in bands 1, 2, and 3, as well as the coefficients in the equation (2). The first 3 elements in R are reflectance values from MOD09 and the last one is 1.00, or the sum of all the types' coverage. The different observations report gave similar values (Grenfell and Gary A., 1977; Tucker et al., 1999; Tschudi et al., 2008) for the coefficient matrix. Finally, Lower-Upper (LU) decomposition is applied to solve the equation set.

In the T08 algorithm, the reflectance coefficients of four types in channels 1 and 3 are close, so the system of linear equations is approximately linearly correlated which causes the ill-conditioned problem to the solution of the reflectance matrix. More specifically, the solutions to the linear equations are sensitive to biases in the input data and result in large numeric errors and computational instability. To detect this problem, the condition number is introduced here as a criterion for the sensitivity of the solution in the system to the error in the input value.

The condition number of the matrix is equal to the product of the norm of the matrix and the norm of the inverse matrix. The smaller the condition number is, the lower the sensitivity of the matrix. By combining 3 bands among 5 visible and near-infrared bands of MODIS data, their respective condition numbers were obtained. And the new band combination with the lowest sensitivity (lowest degree of linear correlation) will be selected.

To improve the algorithm, we introduce pre-processing and also remove one reflectance equation from the original set. And the same condition number process was taken afterwards by combining 2 bands among 5 MODIS bands.

4. RESULT

4.1 Condition numbers for the three-band combination algorithms and the MPF retrieval results

To check the condition numbers of different combinations of three bands, the reflectivity of each surface type for different MODIS bands need to be given first. In table 1, the reflectance coefficients of snow, ice, and melt pond are following T08 based on the in-situ observation near Barrow, Alaska, June 2004, while that of water does not exist in their observation. Here we set them as the mean of reflectance value of the water point selected from different MODIS bands.

Band	Band width (nm)	Melt pond r1	Bare ice r2	Snow r3	Open wate r r4
B1	620-670	0.16	0.75	0.95	0.02
B2	841-876	0.07	0.56	0.87	0.01
B3	459-479	0.22	0.76	0.95	0.04
B4	545-565	0.23	0.76	0.96	0.03
B5	1230-1250	0.04	0.15	0.49	0.01

Table 1. Reflectivity of each surface type for different MODIS bands

The condition numbers of different combinations of three bands are shown in Table 2. The combinations that include both bands 1 and 3 have large condition numbers. The combinations including both bands 3 and 4 are similar, since the reflectance coefficients of four types are even closer to each other for these two bands. Among the left combinations, bands 2,4,5 (B245) has the smallest condition number (74,46,97 under the norm of 1, 2, and ∞). Following are B235 (84,53,112) and B145 (114,77,134).

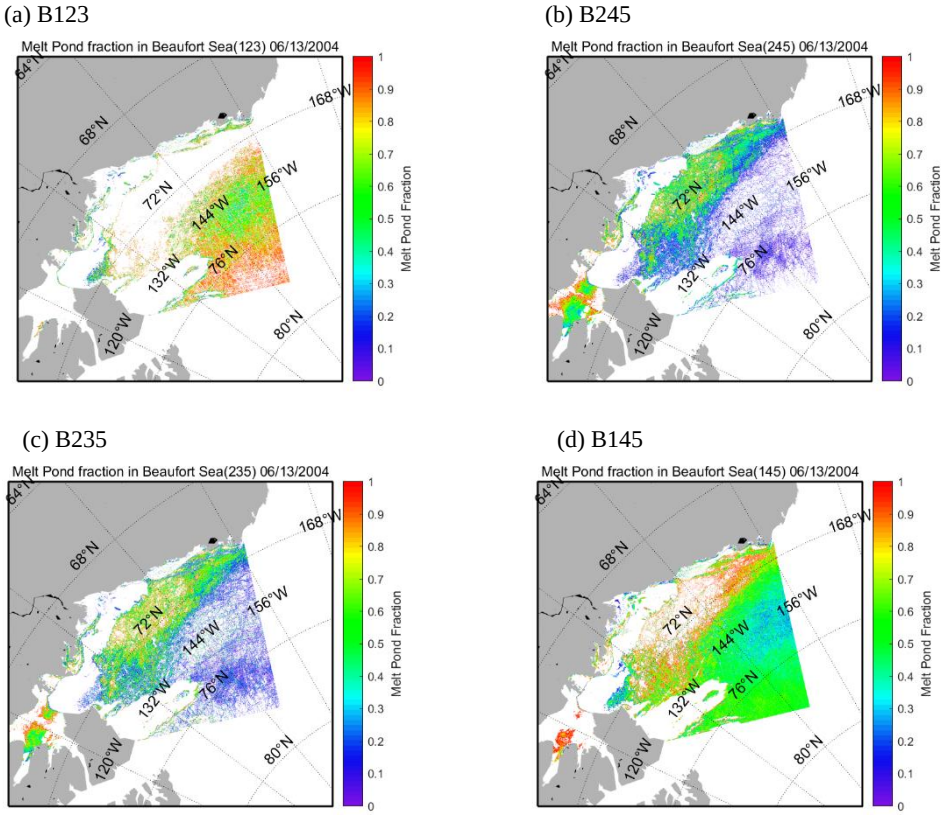

Figure 2. MPF retrieval result using three-band algorithm in different combination

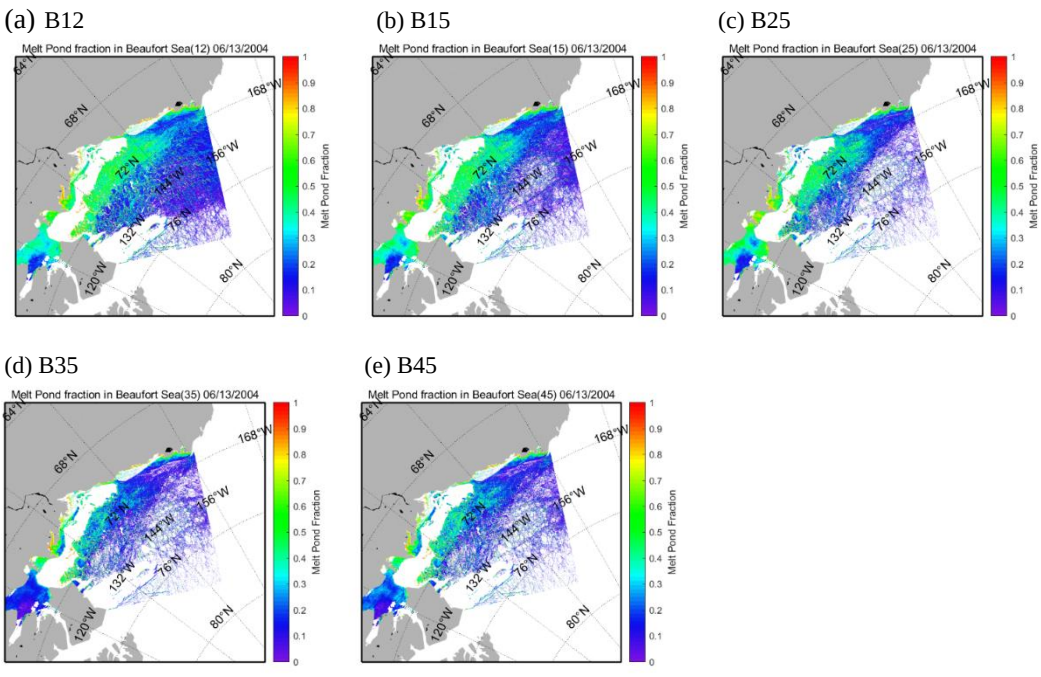

Figure 3 MPF retrieval result using two-band algorithm in different combination

Band	Norm 1	Norm2	Norm∞
B123	284	140	209
B124	198	95	136
B125	129	81	169
B134	1355	785	1398
B135	161	109	193
B145	114	77	134
B234	555	283	388
B235	84	53	112
B245	74	46	97
B345	395	265	469

Table 2. The condition numbers of different combinations of three bands

Figure 2a is MPF derived by the T08 algorithm in the same region as Figure 1. There are several large regions with unrealistic coverage values, for example, the blue band to the southwest of Banks Island is open water in reality, and thus its MPF should be zero rather than values about 0.20. Besides, there is melting sea ice floating to the north of open water, with melt ponds on the ice surface, but coverage values are beyond [0,1] there, which is physically impossible. Accordingly, the MPF algorithm using the above three combinations was applied to MOD09 data. The results show that B245 and B235 give more reasonable MPF than the original T08 combination of B312 (Figure 2b-d).

4.2 Condition numbers for the two-band combination algorithms and the MPF retrieval results

Even for the combination of B245, the conditional number is still between 46 and 97, so there still exists a linear correlation problem. To further reduce the sensitivity of the matrix, the next step is to reduce one equation for the experiment. This means we have to exclude one surface type to make the equation solvable. Here we remove open water by ice-water discrimination based on the reflectance of band 4, which has the largest difference between the reflectance of water and that of other types.

The two-band combination results (Table 3) show that the top three with the low condition numbers are B15 (22,13,22), B35(22,14,23), and B45 (23,14,24). Following B25 (28,17,28) and B12(53,38,59). Furthermore, these five combination algorithms are also applied to MOD09A1 data (Figure 3). It's obvious, all MPF results from the two-band algorithms are lower than that of three-band algorithms.

Band	Norm 1	Norm2	Norm∞
B12	53	38	59
B13	1118	797	1154
B14	383	273	396
B15	22	13	22
B23	61	42	67
B24	68	47	75
B25	28	17	28
B34	582	431	603
B35	22	14	23
B45	23	14	24

Table 3. The condition numbers of different combinations of two bands of MODIS

4.3 Comparison and validation

According to the classification method of Markus et al. (2002, 2003) from Landsat-7ETM+, we discriminate different surface types based on bands 1, 2, and 3 reflectance of Landsat5 TM. Before applying the classification algorithm, atmosphere corrections are conducted using Moderate Resolution Atmospheric Transmission (MOTRAN) transfer model. This aims to reduce the impacts of the atmosphere and gets "near-surface" reflectance values. As a result, we choose the reflectance values from in-situ observations (T08) to replace the original thresholds:

Snow: $r_1 > 0.70$ or $r_2 > 0.70$

Bare ice: $0.12 < r_1 < 0.70$ and $r_3 - r_2 > -0.08$

Melt pond: $r_1 > 0.12$ and $r_3 - r_2 < -0.08$

Open water: $r_1 < 0.12$

where r_1, r_2 and r_3 stand for the reflectance of Landsat Band 1, Band 2 and Band 3, respectively.

Figure 4a shows the combination TrueColor image of B123 from Landsat data. We projected Landsat data onto the MODIS data grid and statistically calculated the proportion of the areas covered by melt ponds by discriminating bare ice, snow, melt pond and water, and the MPF results of classification are shown in Figure 4b. There is an area with relatively high MPF in low left corner of the image.

The comparisons were made between the retrieval MPF of five experiments in section 4.2 and the result from Landsat classification (Figure 5). All the MPF results obtained by the two-band algorithms from MODIS data are smaller in high MPF regions, while relatively larger in low MPF regions than those obtained by surface type discrimination method from Landsat data.

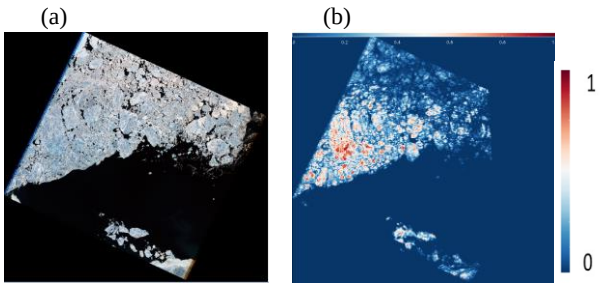

Figure 4 Landsat B123 TrueColor image and the MPF by classification from Landsat data

Table 4 gives the bias between MPF results from five two-band algorithms and that from Landsat data. The result of B15 with the smallest bias from Landsat retrieval result with mean error (ME) as 0.043 and root mean square error (MSE) as 0.142.

Band	ME	MSE
B12	0.165	0.297
B15	0.043	0.142
B25	0.160	0.259
B35	0.062	0.266
B45	0.083	0.262

Table 4. The bias between MPF results from five two-band algorithms and that from Landsat classification

Then the B15 combination algorithm was applied to MOD09A1 data in 2007 spring and summer. The results are approximately consistent with the MPF product of University Hamburg in the distribution and evolution of melt ponds (Figure 6). The main difference between the two algorithms is that our results have a relatively higher MPF in the regions covered by first-year ice, especially in the Pacific sector. Further comparison with aerial photographs and other high-resolution optical data is needed.

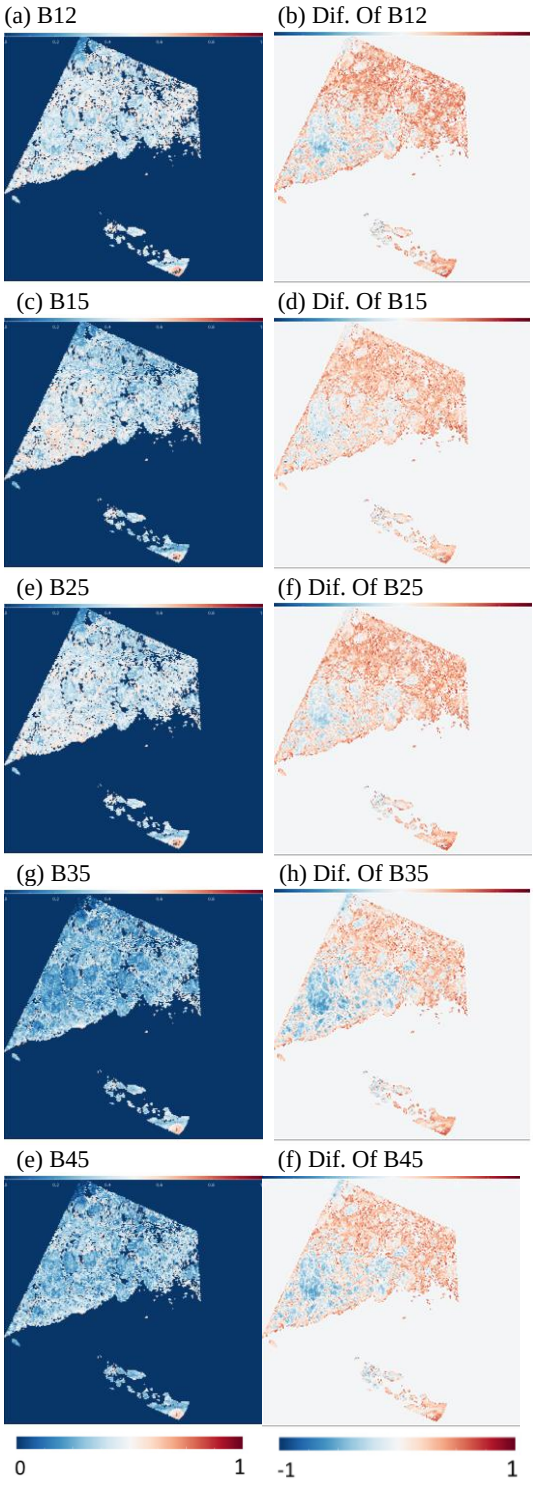

Figure 5. MPF retrieval from two-band algorithms (left panels) and the difference compared with that of Landsat discrimination (right panels)

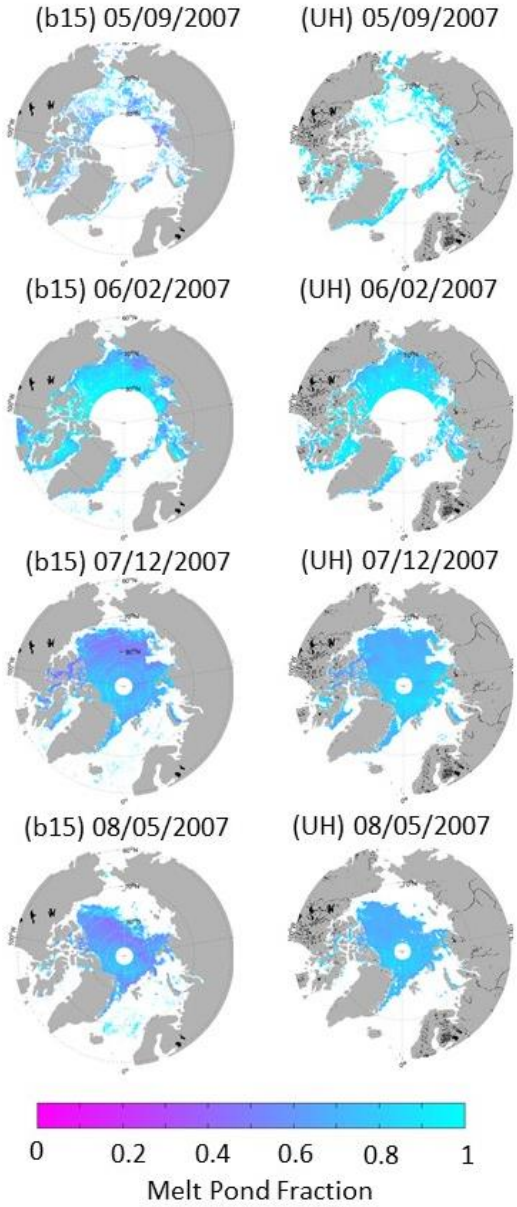

Figure 6 Comparison between MPF from B15 algorithm and that from University Hamburg

5. CONCLUSION AND DISCUSSION

Melt ponds have an important effect on the decrease of Arctic sea ice in summer. Due to their low albedo, they accelerate the positive feedback process of sea ice-albedo. In this paper, we analyse a regional MPF algorithm proposed by T08 algorithm which is based on solving a linear equation set consisting of multi-channel reflectance and area faction. We developed the MPF retrieval algorithm with some experiments to reduce the sensitivity of the linear functions based on MODIS data. Comparison is made with Landsat solutions and the MPF product from University Hamburg. Several conclusions and discussions are summarized as the following.

The solution of linear unmixing equation is very sensitive to input data errors due to its ill-conditioned reflectance matrix. This issue is caused by the strong linear correlation between reflectance vectors of Band 1 and Band 3 in T08's algorithm.

The strong correlation, along with limitations of the earth surface in-situ observation hinders the improvement path of adding new band equations. We propose to improve T08 algorithm by introducing the condition number as well as a pre-processing module (remove open water from surface types) and removing an equation from the original linear system.

The results show that B245 has the smallest condition number and lead to more reasonable estimates of the MPF than the original T08 combination of B123. All the two-band results have lower MPF values in high MPF regions while have larger MPF in low MPF regions than those from three-band algorithms. Among them, B15 has the smallest condition number and also has the smallest bias from the MPF from Landsat discrimination.

The new MODIS algorithm outperforms the original version in reducing unrealistic solutions. It can also generate reasonable MPF distribution over broad area. Further comparison with MPF from University Hamburg shows that the B15 algorithm can generate reasonable outputs across the Arctic basin with a relatively larger value especially in Pacific sector.

The comparisons of results with Landsat-5 TM classification suggest that we still need to enhance the new algorithm's skill in treating some fine-resolution surface features; meanwhile, there may be some biases in the derived MPF values. Investigations that combine in-situ and airborne observations will help to improve the algorithm. We are also working on using airborne images to validate the algorithm.

ACKNOWLEDGEMENTS

This work was supported by the National Key Research and Development Program of China (2018YFA0605903 and 2016YFC1402705).

REFERENCES

Grenfell, T.C., Maykut, G.A., 1977: The optical properties of ice and snow in the Arctic Basin. *J. Glaciol.*, 18, 445-463.

Istomina, L., Heygster, G., Huntemann, M., Marks, H., 2015: Melt pond fraction and spectral sea ice albedo retrieval from MERIS data – Part 1: Validation against in situ, aerial, and ship cruise data. *The Cryosphere*, 9(4), 1551-1566. doi: 10.5194/tc-9-1567-2015.

Landy, J.C., Ehn, J.K., Barber, D.G., 2015: Albedo feedback enhanced by smoother Arctic sea ice. *Geophys. Res. Lett.*, 42, 10714– 10720. doi:10.1002/2015GL066712.

Landy, J.C., Ehn, J.K., Shields, M., Barber, D., 2014: Surface and melt pond evolution on landfast first-year sea ice in the Canadian Arctic Archipelago. *J. Geophys. Res. Oceans*, 119, 3054– 3075. doi:10.1002/2013JC009617.

Lu, P., Li, Z., Cheng, B., Lei, R., Zhang, R., 2010: Sea ice surface features in Arctic summer 2008: Aerial observations. *Remote Sens. Environ.*, 114(4), 693-699. doi: 10.1016/j.rse.2009.11.009.

Markus, T., Cavalieri, D.J., Ivanoff, A., 2002: The potential of using Landsat 7 ETM+ for the classification of sea-ice surface conditions during summer. *Ann. Glaciol.*, 34(1), 415-419. doi:10.3189/172756402781817536.

Markus, T., Cavalieri, D.J., Tschudi, M.A., Ivanoff, A., 2003: Comparison of aerial video and Landsat 7 data over ponded sea ice. *Remote Sens. Environ.*, 86, 458-469. doi: 10.1016/s0034-4257(03)00124-x.

Perovich, D.K., Tucker, W.B., Ligett, K.A., 2002: Aerial observations of the evolution of ice surface conditions during summer. *J. Geophys. Res.*, 107(C10), 8048. doi:10.1029/2000JC000449.

Polashenski, C., Perovich, D.K., Courville, Z., 2012: The mechanisms of sea ice melt pond formation and evolution. *J. Geophys. Res.*, 117, C01001. doi:10.1029/2011JC007231.

Rösel, A., Kaleschke, L., 2011: Comparison of different retrieval techniques for melt ponds on Arctic sea ice from Landsat and MODIS satellite data. *Ann. Glaciol.*, 52(57), 185-191. doi: 10.3189/172756411795931606.

Rösel, A., Kaleschke, L., Birnbaum, G., 2012: Melt ponds on arctic sea ice determined from MODIS satellite data using an artificial neural network. *The Cryosphere*, 6(2), 431-446. doi:10.5194/tc-6-431-2012.

Tschudi, M.A., Curry, J.A., Maslanik, J.A., 2001: Airborne observations of summertime surface features and their effect on surface albedo during FIRE/SHEBA. *J. Geophys. Res.*, 106(D14), 15335-15344. doi:10.1029/2000JD900275.

Tschudi, M.A., Maslanik, J.A., Perovich, D.K., 2008: Derivation of melt pond coverage on Arctic sea ice using MODIS observations. *Remote Sens. Environ.*, 112(5), 2605-2614. doi:10.1016/j.rse.2007.12.009.

Tucker, W.B., Gow, A.J., Meese, D.A., Bosworth, H.W., Reimnitz, E., 1999: Physical characteristics of summer sea ice across the Arctic Ocean. *J. Geophys. Res.*, 104, 1489-1504. doi:10.1029/98JC02607.

Zege E., Malinka, A., Katsev, I., Prikhach, A., Heygster, G., Istomina, L., Birnbaum, G., Schwarz, P., 2015: Algorithm to retrieve the melt pond fraction and the spectral albedo of Arctic summer ice from satellite optical data. *Remote Sens. Environ.*, 163,153-164. doi:10.1016/j.rse.2015.03.012.